ORIGINAL PAPER

Migration of organic compounds from PET/clay nanocomposites: influences of clay type, content and dispersion state

Siamak Motahari · Lida Dornajafi ·
Iman Fotovat Ahmadi

Abstract Polyethylene terephthalate (PET) bottles are widely used for packaging mineral water or soft drinks. Migration of toxic residual phthalate esters from PET could potentially change the quality of the bottled contents. The main purpose of this study is to control the migration of five different phthalate esters from PET bottles into the water they contained. To achieve this goal, three different types of nanoclay particles were added to PET to slow down the migration of the toxic phthalate esters. The concentration of phthalate esters in the water in contact with PET and PET/nanoclay was measured by gas chromatography (GC-FID) combined with the directly suspended droplet microextraction method. Good precision, accuracy and reproducibility over a wide linear range were achieved by the proposed technique under optimal conditions. The experimental results reveal that adding nanoclay fillers to the PET decreases the release of the above-mentioned chemicals from PET into the water considerably due to attainment of a tortuous diffusive path. Data also indicate the significant effect of nanoclay volume fraction and exfoliated morphology on obtaining efficient barrier properties. Furthermore the effects of parameters such as storage time, temperature, and amount and type of nanoclay inclusions were studied on the migration rate, as well.

Keywords Nanocomposites · Polyethylene terephthalate · Directly suspended droplet microextraction · Gas chromatography · Barrier properties

S. Motahari (✉) · L. Dornajafi · I. Fotovat Ahmadi
School of Chemical Engineering, College of Engineering,
University of Tehran, P.O. Box: 11155-4563, Tehran, Iran
e-mail: smotahari@ut.ac.ir

Introduction

The increasing demand for versatile properties, such as good impact resistance, chemical resistance, transparency, being light weight and possibility of recycling in food, beverages and cosmetic packaging industries, have made polyethylene terephthalate (PET) one of the most widely applied thermoplastics. However, it should be noticed that diffusion and migration of by-products, catalysts, additives as well as hydrolysis and thermal degradation residues of either virgin or recycled PET into food or water may contaminate its content. Phthalate esters are potential migrant compounds which are not covalently bound to plastic materials [1]. Their presence and migration from PET into water and foods have been investigated by several authors [2–6]. Prokupková et al. [5] showed the presence of various phthalate esters including dimethyl phthalate (DMP) diethyl phthalate (DEP), dibutyl phthalate (DBP), and bis 2-ethylhexyl phthalate (DEHP) in water and concluded that the type of packaged material could affect the concentrations of these esters. Rios et al. [7] analyzed olive oils that were kept in a PET containers for several months and determined the presence of DBP, DEHP, benzyl butyl phthalate (BBP) and di-iso butyl phthalate (DIBP) in the samples, but none of DMP and DEP was detected. Substantial considerations have been given to the influence of phthalate esters on human health recently due to their potential toxicity [8, 9]. Scientific researches have shown that phthalate esters may adversely affect the human body and impair human fertility comprising a reduction in the level of sex hormones in both genders [10–13]. Bearing in mind their potential risks to human health and the environment, these phthalates are on the first three priority lists for risk assessment in accordance with the European Union's Regulation 793/93 on existing substances. The US

Environmental Protection Agency (EPA) has set the maximum contamination level (MCL) for DEHP in water systems at 6 $\mu g\ L^{-1}$ and recommended that concentrations above 0.6 $\mu g\ L^{-1}$ be closely monitored. Simultaneously, US EPA advises close screening of phthalate in drinking water at concentrations above this limit. Moreover, other compounds such as DBP and DEP have been included in the third contaminant candidate list for compounds that may require regulations under the Safe Drinking Water Act (criterion of 3 $\mu g\ L^{-1}$) [6]. Therefore, decreasing the level of migration of phthalate esters from PET into packaging water and foods is absolutely essential.

Nowadays, particular attention has been paid to nano-scale particles due to their low volume fractions and great impact on diverse characteristics of the polymers compared with conventional microparticle additives. Among various nanoparticles that have been introduced, packaging industries have concentrated primarily on layered nanoclays such as montmorillonite (MMT) due to their low cost, availability, and also because these are environmentally friendly [14, 15]. However, some researchers believe that the minor disadvantage of nanoclay particles is the reduction of transparency and optical transmission [14, 16].

Dispersion efficiency of the most commonly used silicate layers known as nano-montmorillonite particles in polymer matrices is critical in order to achieve improved properties. However, dispersion of organophobic silicate layers of natural MMT in organic polymer matrix is not simple and needs proper revision. Therefore, modifications are performed on natural MMT interlayers to form organically modified nano-montmorillonite (OMMT) with the purpose of enhancing their compatibility and interaction with polymer chains. It also helps to increase the interplanar spacing of the layered silicates to easily delaminate and to form intercalated and exfoliated structures. Polymer chains may penetrate between silicate layers and increase their gallery spacing distance. In this case, intercalated structures are formed. A comprehensive penetration causes the interlayer to be taken apart and creates exfoliated structures in which individual platelets are dispersed homogeneously.

Nanocomposites with an exfoliated morphology are preferred because of their high level of strength, stiffness, thermal stability and optimal interaction between platelets of nanoclay and polymer [17–20]. Different methods can be used to process PET/nanoclay nanocomposites which mainly involve solution intercalation, in situ polymerization and melt compounding. Nevertheless, melt compounding technique seems to be more popular because of its versatility, convenience, compatibility with other polymer processes, economic advantages and the absence of any solvents. [15, 20–22].

Several studies have been devoted to the effects of nanoclays on typical barrier properties of different polymers including polyesters, polyvinyl chloride (PVC), polyvinyl acetate (PVA), polyimides, polyurethanes, high-density polyethylene (HDPE), polylactic acid, polyureas and epoxy resins [20, 23, 24].

Xu et al. [25] Concluded that the relative permeability of polymer/clay nanocomposites depends mostly on the clay layers' dispersion, thickness and length, gallery spacing, layer volume fraction and the chain segment immobility factor. It was also reported that gas barrier properties of PET nanocomposite containing 1 wt% of well-dispersed OMMT improved as the oxygen transmission rate reduced to half in comparison with pure PET [26]. Based on a review study, different studies have revealed the decrease in oxygen permeation from PET/clay nanocomposites compared to that of pure PET [20]. However, most of the performed studies are related to the transmission of small gases such as O_2, N_2, He, CO_2 or water vapor from nanocomposites and their barrier properties. In fact, there are limited studies focused on the migration of residues and contaminants from polymer/clay nanocomposites.

The main objective of the present work is to investigate the impact of three different kinds of nanoclays on the level of phthalate esters migration from polyethylene terephthalate (PET) into bottled water. The potential release of these endocrine disruption compounds into water samples stored in diverse conditions was also explored. The different chemical nature of the natural MMT and OMMTs also allows us to determine the characteristics of the nanoclay particles that lead to various dispersion states in PET-based clay nanocomposites.

Experimental

Materials

Bottle-grade polyethylene terephthalate (PET6801, intrinsic viscosity (IV) = 0.82 dL g^{-1}) was supplied from Hualon Co., Korea, the properties of which are listed in Table 1. Three different types of montmorillonite nanoparticles (Cloisite Na$^+$, Cloisite 15A, and Cloisite 30B) were supplied from Southern Clay Products, USA, with the properties listed in Table 2. Phthalate esters including dimethyl phthalate (DMP), diethyl phthalate (DEP), dibutyl phthalate (DBP), diisobutyl phthalate (DIBP) and bis-2ethylhexyl phthalate (DEHP) were purchased from Merck (Darmstadt, Germany). Triple-distilled water was used throughout the experiments. Other chemicals were purchased from Merck.

Table 1 Characteristics of polyethylene terephthalate (PET)

PET Hualon 6801

Inherent viscosity (dL/g)	Melting temperature (°C)	Acetaldehyde (ppm)	COOH end groups (Ueq/g)	Moisture (ppm)	Crystallinity (%)
0.82 ± 0.02	245	<1	<30	<100	>40

Table 2 Comparison of the properties of Cloisite Na$^+$, Cloisite 15A and Cloisite 30B

	Clay type	Organic modifier	Cation exchange capacity (CEC)	Density (g/cm^3)	d-Spacing (d$_{001}$) (Å)	Particle size range (μm)	Moisture (%)
Cloisite Na$^+$	NaMMT^a	–	92 meq/100 g clay	2.86	11.7	2–13	4–9
Cloisite 15A	OMMT^b	2M2HT^c	125 meq/100 g clay	1.66	31.5	2–13	<2
Cloisite 30B	OMMT	MT2EtOH^d	90 meq/100 g clay	1.98	18.5	2–13	<2

^{a} Na$^+$ montmorillonite; ^{b} organically modified montmorillonite; ^{c} dimethyl dehydrogenated tallow, quaternary ammonium chloride; ^{d} methyl tallow bis -2-hydroxyethyl, quaternary ammonium chloride

Table 3 Applied weight fraction and volume fraction of different nanoclays used for the preparation of nanocomposites

	Weight fraction (%)	Volume fraction (%)
Cloisite Na$^+$	2	0.97
	4	1.96
Cloisite 15A	2	1.66
	4	3.33
Cloisite 30B	2	1.39
	4	2.8

Table 4 Properties of various phthalate esters analytes

Analytes	Molecular formula	Molar mass (g/mol)	Density (g/cm^3)	Boiling point (°C)	Flash point (°C)
DMP	$C_{10}H_{10}O_4$	194.184	1.19	283	146
DEP	$C_{12}H_{14}O_4$	222.24	1.12	295	117
DiisoBP	$C_{16}H_{22}O_4$	278.35	1.038	320	185
DBP	$C_{16}H_{22}O_4$	278.34	1.05	340	157
BEHP	$C_{24}H_{38}O_4$	390.56	0.985	385	207

Preparation of nanocomposites

Melt compounding of PET with sodium montmorillonite (NaMMT) and OMMT particles was performed using an internal mixer. Previously, PET granules were dried for 8 h at 120 °C under vacuum. Nanoclays including NaMMT and OMMT were also dried at 80 °C for 12 h under vacuum. Nanocomposite samples were melt blended in co-rotating twin screw internal mixer (Brabender) at 265 °C for 6 min with rotor speed of 60 rpm to achieve proper mixing. PET/nanoclay samples with clay content of 2 and 4 wt% were prepared using Cloisite Na$^+$, Cloisite 30B and Cloisite 15A. The weight and volume fraction of nanoclay fillers in the polymer matrix are displayed in Table 3.

Sheets of each prepared sample with 0.5 mm thickness were obtained by compression molding at 260 °C for 1 min under a pressure of 700 kPa. Then, 0.5 g of each of prepared and pristine PET samples were cut to 1 × 1 mm pieces and put in 14 mL of distilled water at two exaggerated storage temperatures, 7 °C and 45 °C, to survey the migration of phthalate esters. Migration experiments were also carried out at two different time intervals, 4 weeks and 6 weeks. Properties of the phthalate esters migrants are presented in Table 4.

X-ray diffraction

X-ray diffraction (XRD) can be utilized to characterize the extent of intercalation and exfoliation of nanoclay platelets. XRD experiments were performed using Philips X'pert MPD diffractometer (The Netherlands) at room temperature in refraction mode. CuK$_\alpha$ radiation operated at 40 mA and 40 kV was used with diffraction angle 2θ ranging from 1° to 10°.

Gas chromatography analysis

The amount of phthalate ester analytes in water samples was determined using gas chromatography (GC) analysis coupled with directly droplet microextraction (DSDME) technique. GC analyses were performed using a Varian CP-3800 series gas chromatograph (USA) equipped with split/splitless injector and flame ionization detector (FID). Separation capillary column used was a DB-1 with
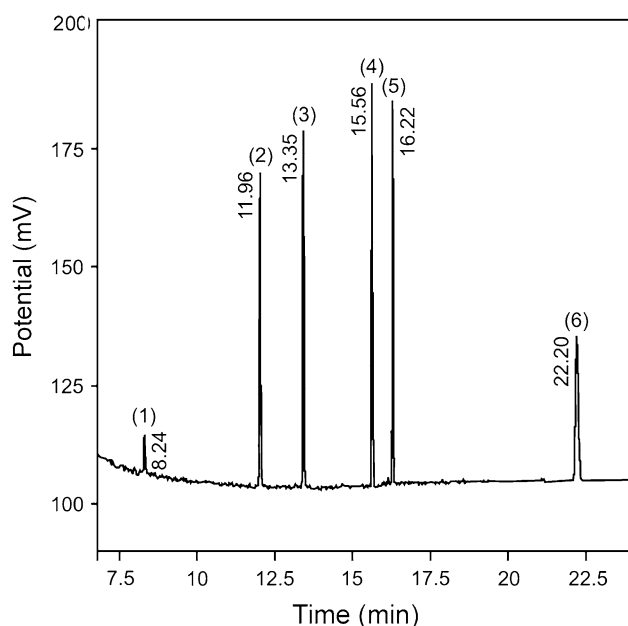
Fig. 1 GC-FID chromatographs of standard solutions of phthalate esters (100 µg mL^{-1}) and their retention times: (*1*) Internal Standard, (*2*) DMP, (*3*) DEP, (*4*) DIBP, (*5*) DBP and (*6*) DEHP

30 m × 0.25 mm internal diameter and 0.25 µm coated thickness. For all analyses the injections were performed in splitless mode. Oven temperature was programmed initially at 90 °C for 2 min, increasing to 180 °C at the rate of 10 °C min^{-1} and then it was raised to 265 °C at the rate of 15 °C min^{-1} and kept at this final temperature for 10 min. Detector and injector temperature were arranged to 300 °C and 265 °C, respectively. Flow rate of the helium as carrier gas was 7 mL min^{-1}. FID was fed by synthetic air (350 mL min^{-1}) and hydrogen (35 mL min^{-1}).

Preparation of standard solutions

Stock solutions of analytes (1,000 µg mL^{-1}) were prepared in ethyl acetate and stored at 4 °C. Standard solutions of phthalate esters in ethyl acetate with 1, 5, 10 and 100 µg mL^{-1} concentrations were prepared by diluting the stock solution. An amount of 100 µL of ethyl benzoate with constant concentration of 1,000 µg mL^{-1} was added as internal standard. To determine the linearity of the response, 2 µL of the above four concentrations was each injected for three times into the GC unit. A chromatograph of standard solution of phthalates (100 µg mL^{-1}) and their retention times is presented in Fig. 1. Peak surface ratios of each analyte to internal standard peak surface were used to draw the calibration curves. The calculated calibration curves gave a high level of linearity in the range of 1–100 µg mL^{-1} for all target analytes with correlation coefficients ranging between 0.9991 and 1. Repeatability, expressed as a percentage of coefficients of variation (CV%), was lower than 9.86 %. Limit of detection (LOD) and limit of quantification (LOQ) values were calculated on the basis of calibration curve slopes and standard deviation of the blank sample responses that was injected three times. The first value was obtained between 0.42 and 1.01 µg mL^{-1} and the second one between 1.4 and 3.36 µg mL^{-1}.

Directly suspended droplet microextraction

According to the presentation of low concentration of analytes in aqueous solutions, directly suspended droplet microextraction (DSDME) technique was employed to bring the analytes to a suitable concentration level. Furthermore, by this method, the aqueous solutions were replaced with organic solutions, and thus they could be directly detected by GC. In this method, a stirring bar is placed at the bottom of the aqueous sample rotating at an appropriate speed by means of a magnetic stirrer which causes a weak gentle vortex in the solution. The needle of a 10 µL microsyringe (Hamilton, Bonaduz AG, Bonaduz Switzerland) was then inserted through the cylindrical vial (20 mm diameter) and immersed in the aqueous feed solution. A small volume of an immiscible organic solvent is added to the surface of the solution and hence motion of the vortex results in the formation of a single micro-drop at or near the center of rotation.

To make a steady vortex, it is important to keep the stirring bar rotating smoothly just at the center of the base. The droplet itself may also rotate on the surface of the aqueous phase, increasing mass transfer. Then, the syringe was removed and the screw cap of the vial was replaced. Compared with the other liquid phase microextraction (LPME) technique, DSDME provides more flexibility in the choice of the operational parameters. The possibility of using larger volumes of organic solvent in this method in addition to GC makes it a useful technique comparable to HPLC [27].

To increase the enrichment factor and to achieve good droplet stability, factors such as organic solvent, stirring speed and solvent volume must be optimized. The solvent should have good affinity for target compounds, low solubility in water such as to prevent the dissolution in the aqueous phase and lower density than water. Thus, benzene, toluene and ethyl acetate were tested as organic extraction solvents, and more stable droplets and higher extraction efficiency were achieved when toluene was applied. In smaller droplets, the area to volume ratio is greater than the larger ones. Therefore, mass transfer can take place more easily in a smaller size droplet. In addition, the enrichment factor has a reverse correlation with ratio of organic to aqueous phases.

Among the three studied solvent volumes (20, 24, and 50 µL), 24 µL of toluene was used to extract analytes from
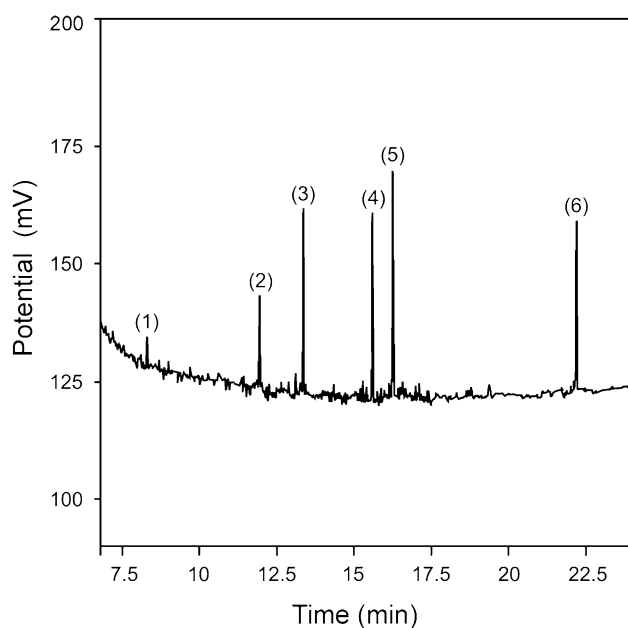
Fig. 2 GC-FID chromatographs of phthalate solutions (100 ng mL^{-1}) after the microextraction procedure: (*1*) Internal Standard, (*2*) DMP, (*3*) DEP, (*4*) DIBP, (*5*) DBP and (*6*) DEHP

14 mL of water samples due to higher extraction efficiency as a result of reaching equilibrium in the proper microextraction time (30 min) as well as providing more steady droplets during agitation. Stirring speed also has a direct influence on both the shape of the droplet and the mass transfer characteristics in the aqueous sample. It was observed that stirring rates above 1,050 rpm caused instability and displacement of the organic droplet. Hence, a stirring speed of 1,050 rpm was selected for implementing DSDME in ambient temperature. No salt was added to the aqueous solution. Utilizing optimized parameters, the extracted droplets (2 μL) were drawn into the microsyringe and after 2 min the collected sample was injected directly into GC unit for further analyses.

Results and discussion

Method of validation

To evaluate the practical applicability of the extraction technique and its linearity, repeatability, reproducibility and limit of detection in distilled water, samples spiked at ng mL^{-1} concentration levels of phthalate esters were investigated. Aqueous solutions of analytes with concentration range 1–100 ng mL^{-1} were prepared and extracted under the aforementioned optimal extraction conditions. For each concentration, three replicate extractions were

performed. The injected volume of the extracted analytes into GC was kept constant at 2 μL. A chromatograph of phthalate solution with spiking level of 100 ng mL^{-1} after microextraction is shown in Fig. 2. Calibration curves were obtained by plotting the peak area of the analytes versus their corresponding concentrations in spiked water samples. The linearity of the calibration curve was evaluated using least-squares linear regression analysis.

As summarized in Table 5, all the target analytes exhibited a high level of linearity over the concentration range studied (1–100 ng mL^{-1}). Correlation coefficients (R^2) were satisfactory, being greater than 0.9974 for all the studied analytes. To assess the precision of the measurement, the repeatability of the method was determined by extracting three aqueous samples spiked at five different concentration levels with each target analyte (Table 6). The coefficients of variation for the spiked samples did not exceed 9.90 %, which indicates that the developed method is precise.

Reproducibility was carried out by analyzing the samples with similar spiking level in consecutive days with three replications and its results are presented in Table 6. The obtained values of LOD (0.85–1.82 ng mL^{-1}) and LOQ (2.83–6.06 ng mL^{-1}) demonstrate the high sensitivity of the method. In fact, the presented method is capable of detecting and quantifying phthalate ester concentrations below the maximum permitted residue level. The wide linear range combined with the low detection limits obtained with the proposed extraction method suggests a high potential for monitoring phthalate esters in water samples.

Enrichment factor values reveal the efficiency of the proposed extraction method. To investigate the matrix effect and applicability of the procedure, experiments were carried out on tap water samples with similar spiking level of analytes, and the obtained relative recoveries show no significant interference of matrix (Table 6). Results confirm that the method is highly selective and sensitive enough to allow determination of ng mL^{-1} concentration of phthalate esters in different matrices. It is free of cross contamination and has very low solvent consumption as well as high extraction efficiency.

X-ray diffraction analysis

Gallery spacing distance (d$_{001}$), diffraction angle (2θ), and maximum peak intensity for Cloisite Na$^+$, Cloisite 30B, and Cloisite 15A were determined by Bragg's law from XRD patterns (Table 7). Gallery spacing distance indicated good correlation with the manufacturer's data (Table 2). Cloisite 15A possesses higher level of gallery spacing and

Table 5 Linearity range, calibration data and other quantitative results of DSDME and GC-FID

Analyte	Linearity range (ng mL^{-1})	Regression equation	Correlation coefficient (R^2)	EF[a]	LOD (ng mL^{-1})	LOQ (ng mL^{-1})
DMP	1–100	$y = 0.0055x + 0.139$	0.9994	627	1.52	5.06
DEP	1–100	$y = 0.0063x + 0.2005$	0.9986	598	1.82	6.06
DIBP	1–100	$y = 0.007x + 0.1713$	0.9986	379	1.48	4.93
DBP	1–100	$y = 0.007x + 0.1456$	0.9974	658	1.14	3.8
DEHP	1–100	$y = 0.0508x + 1.0117$	0.9990	345	0.85	2.83

[a] Enrichment factor

Table 6 Repeatability, reproducibility and relative recoveries of phthalate esters by the DSDME technique

Analyte	Repeatability (CV%)[a]					Reproducibility (CV%)[b]	Relative recovery (%)[c]
	1	5	10	20	100	10 (ng mL^{-1})	
DMP	8.21	9.16	2.62	7.89	7.77	6.12	97.68
DEP	3.69	8.60	3.40	6.40	9.24	5.51	86.96
DIBP	5.18	9.91	3.65	6.31	5.35	5.40	93.85
DBP	6.78	6.89	3.66	6.91	3.50	5.84	103.61
DEHP	7.08	4.24	4.04	5.94	3.08	5.39	83.16

[a] Sample spiked at five concentrations (ng mL^{-1}); [b] Samples spiked at 10 ng mL^{-1}; [c] Tap water at spiking level 10 ng mL^{-1}, $n = 3$ replicates

Table 7 XRD data for Cloisite Na$^+$, Cloisite 30B and Cloisite 15A, including their characteristic peak intensity, gallery spacing distance (d_{001}) and diffraction angle (2θ) using their XRD patterns
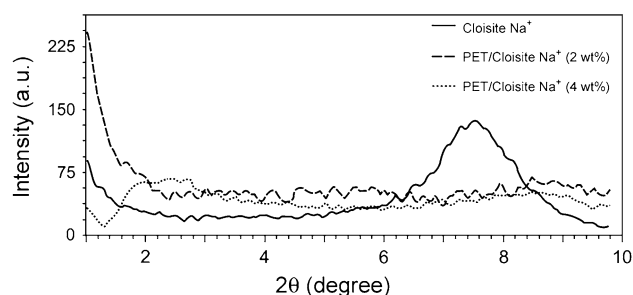
XRD Characteristics	Cloisite Na$^+$	Cloisite 30B	Cloisite 15A
2θ (°)	7.5	5.1	3.08
Peak Intensity (a.u.)	138	435	375
Spacing distance (Å)	12.8	18.8	32.7

Fig. 3 XRD patterns of Cloisite Na$^+$, PET/Cloisite Na$^+$ nanocomposite with 2 wt% nanoclay content and PET/Cloisite Na$^+$ nanocomposite with 4 wt% nanoclay content

modifier concentration compared to the other two types of nanoclays.

PET/Cloisite Na$^+$

X-ray diffraction patterns of PET/Cloisite Na$^+$ nanocomposite samples with 2 and 4 wt% of nanofiller content indicate that the peak at $2\theta = 7.5°$, detected in Cloisite Na$^+$ XRD pattern, has been dissipated (Fig. 3). In other words, the delamination of the Cloisite Na$^+$ nanoclay particles in PET matrix and the increase of interlayer gallery spacing between platelets occurred, which means the formation of exfoliation and intercalation structures in the nanocomposite. In fact, PET chains penetrate into the Cloisite Na$^+$ platelets and increase the clay interlayer distance and this is accompanied by the delamination of stacked layered fillers. Hence, the formation of mixed intercalation-exfoliation structures in 2 wt% Cloisite Na$^+$/PET nanocomposites is assumed.

According to the XRD patterns in Fig. 3, increasing the content of Cloisite Na$^+$ to 4 wt%, leads to lower extent of exfoliated structures as compared to the nanocomposite with 2 wt% nanoclay content. Characteristic peak of Cloisite Na$^+$ at $2\theta = 7.5°$ is shifted to lower angle value ($2\theta = 2.43°$) and also the intensity of the peak is decreased which corresponds to the expansion of gallery spacing and breakdown of agglomerated particles that lead to the formation of intercalation-exfoliation structures.

PET/Cloisite 30B

XRD patterns of pure Cloisite 30B and PET/Cloisite 30B nanocomposite samples with 2 and 4 wt% of nanofiller content are shown in Fig. 4. It is observed that random dispersion of nanoparticles in polymer matrix and formation of exfoliated morphology occurred at lower filler content, i. e., 2 wt% of Cloisite 30B. This can be attributed
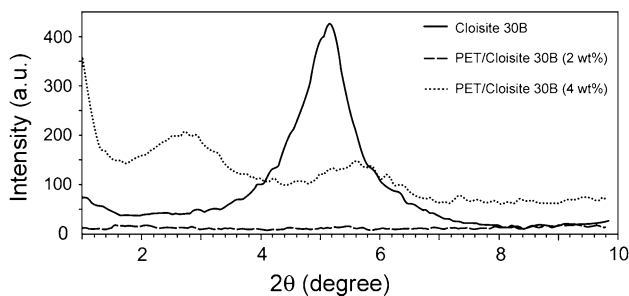
Fig. 4 XRD patterns of Cloisite 30B, PET/Cloisite 30B nanocomposite with 2 wt% nanoclay content and PET/Cloisite 30B nanocomposite with 4 wt% nanoclay content
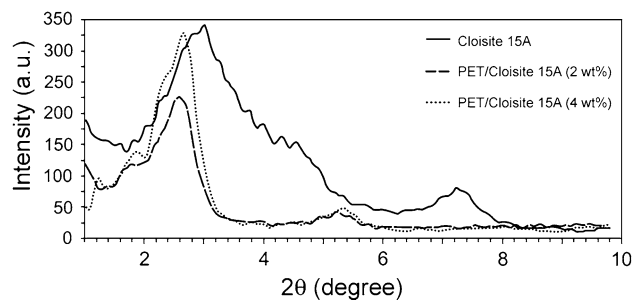

Fig. 5 XRD patterns of Cloisite 15A, PET/Cloisite 15A nanocomposite with 2 wt% nanoclay content and PET/Cloisite 15A nanocomposite with 4 wt% nanoclay content

to the presence of polar modifiers in the Cloisite 30B interlayers, which facilitates the penetration of PET chains into interlayer spaces. Therefore, no diffraction peaks are observed as a consequence of disordering the regular stacks of nanoclay layers during the shear mixing process.

Disappearance of characteristic peak at $2\theta = 5.1°$ with high intensity in XRD pattern of pure Cloisite 30B and formation of two new broader peaks at $2\theta = 2.7°$ and $2\theta = 5.6°$ with lower intensity corresponding to PET/Cloisite 30B with 4 wt% nanoclay content are observed in Fig. 4. This is due to the existence of both intercalated and exfoliated morphology in PET matrix by incorporation of higher Cloisite 30B loading. The increase in nanoclays loading in PET/nanoclay nanocomposites leads to weaker dispersion of nanofillers in polymer matrix and more agglomerate formation. It seems easier to obtain a better dispersion with a low mass fraction of nanoclay due to the less steric effect.

Strong interaction between functional groups of PET molecules and hydroxyl groups of Cloisite 30B considerably promote the penetration of organic chains into the silicate layers to create a well-exfoliated structure, accordingly. It was reported that the polarity of the modifier affects the interfacial interactions and the nanoclay dispersion [28]. More polar nature of Cloisite 30B in comparison to Cloisite 20A facilitated its interaction with polar polytrimethylene terephthalate (PTT) and therefore higher intercalation was achieved [29]. It is also noticed that due to reduction of unfavorable interaction between polymer chains and lone and long alkyl groups of modifier in Cloisite 30B, diffusion of organic chains into interplanar spacing is more convenient [30].

PET/Cloisite 15A

XRD patterns for pristine Cloisite 15A and PET/Cloisite 15A nanocomposites with 2 and 4 wt% nanofiller content have been illustrated in Fig. 5. A peak with low intensity at $2\theta = 7.23°$ corresponding to Cloisite 15A shows that it contains some non-modified nanoclay in its compound,

which means the existence of a small amount of natural MMT in organically modified Cloisite 15A [30–32]. As can be seen, the disordering of the nanoclay layers was not achieved as much as that of nanocomposites containing Cloisite Na$^+$ and Cloisite 30B. In PET/Cloisite 15A with 2 wt% nanoclay content, the peak at $2\theta = 2.68°$ reveals that the shear mixing process has partly dispersed nanoparticles in the PET matrix and the separation of the stacked layers is not fulfilled. Similar trend is seen for nanocomposites containing 4 wt% Cloisite 15A. However, the peak intensity is higher in accordance with lower nanoclay content, which implies weaker dispersal of 4 wt% nanofillers and higher number of aggregated nanoparticles in the PET matrix. The characteristic peak of Cloisite 15A at $2\theta = 3.08°$ is dislocated to $2\theta = 2.7°$ which means that a very slight increase of gallery spacing was obtained. It is also observed that the characteristic peak of the Cloisite 15A becomes narrower, which indicates the presence of tactoids [30]. Nevertheless, XRD patterns in Fig. 5 show that intercalated morphologies exist in PET/Cloisite 15A with both 2 and 4 wt% nanoclay loading.

Cloisite 15A is modified by a non-polar cationic modifier. These non-polar sites on silicate layers of Cloisite 15A are not able to interact with moderately polar PET chains and decrease the entropy of the interlayers. Thus, the delamination of nanoclay platelets does not occur as there is no considerable change in d-spacing of the clay platelets according to XRD patterns in Fig. 5. Although Cloisite 15A contains the highest gallery spacing allowing easier diffusion of the PET molecules into silicate interlayers, intercalation structures are mostly formed due to lack of affinity and polarity interaction between PET and Cloisite 15A. Calcagno et al. [30] announced that the aforementioned behavior of Cloisite 15A in PET matrix originates from unfavorable interaction among polar groups of polymer chains and non-polar groups of the clay particles, as well as their steric hindrance due to the existence of long alkyl groups in their structures.

Table 8 Concentration of migrated phthalate esters in water samples at 7 °C after 4 weeks (ng mL^{-1})

Analyte	PET	2 % PET/Na$^+$	4 % PET/Na$^+$	2 % PET/15A	4 % PET/15A	2 % PET/30B	4 % PET/30B
DMP	71.14	6.4	n.d.	5.12	n.d.	7.72	n.d.
DEP	24.1	n.d.	n.d.	n.d.	n.d.	n.d.	n.d.
DIBP	n.d.	n.d.	n.d.	n.d.	n.d.	n.d.	n.d.
DBP	95.31	11.76	0.62	11.71	n.d.	n.d.	n.d.
DEHP	n.d.	n.d.	n.d.	n.d.	n.d.	n.d.	n.d.

n.d. not detected

Table 9 Concentration of migrated phthalate esters in water samples at 7 °C after 6 weeks (ng mL^{-1})

Analyte	PET	2 % PET/Na$^+$	4 % PET/Na$^+$	2 % PET/15A	4 % PET/15A	2 % PET/30B	4 % PET/30B
DMP	92.2	7.1	5.92	6.57	n.d.	8.9	n.d.
DEP	28.08	n.d.	n.d.	n.d.	n.d.	n.d.	n.d.
DIBP	n.d.	n.d.	n.d.	n.d.	n.d.	2.1	n.d.
DBP	112.4	12.91	1.1	13.34	2.49	3.11	n.d.
DEHP	13.98	n.d.	n.d.	n.d.	n.d.	n.d.	n.d.

n.d. not detected

Table 10 Concentration of migrated phthalate esters in water samples at 45 °C after 4 weeks (ng mL^{-1})

Analyte	PET	2 % PET/Na$^+$	4 % PET/Na+	2 % PET/15A	4 % PET/15A	2 % PET/30B	4 % PET/30B
DMP	89.48	17.35	n.d.	11.84	n.d.	14.42	1.95
DEP	28.62	n.d.	n.d.	n.d.	n.d.	n.d.	n.d.
DIBP	n.d.	n.d.	n.d.	n.d.	n.d.	n.d.	n.d.
DBP	103.9	21.34	6.21	13.62	2.1	14.62	2.05
DEHP	18.21	n.d.	n.d.	n.d.	n.d.	n.d.	n.d.

n.d. not detected

Table 11 Concentration of migrated phthalate esters in water samples at 45 °C after 6 weeks (ng mL^{-1})

Analyte	PET	PET/Na$^+$ (2 wt%)	PET/Na$^+$ (4 wt%)	PET/15A (2 wt%)	PET/15A (4 wt%)	PET/30B (2 wt%)	PET/30B (4 wt%)
DMP	109.62	19.1	3.51	12.48	n.d.	16.51	3.22
DEP	29.17	n.d.	n.d.	n.d.	n.d.	n.d.	n.d.
DIBP	16.2	n.d.	n.d.	n.d.	n.d.	n.d.	n.d.
DBP	126.45	25.36	5.91	15.64	3.25	22.87	2.82
DEHP	27.98	n.d.	n.d.	n.d.	n.d.	n.d.	n.d.

n.d. not detected

Gas chromatography analysis

The amounts of different phthalate esters migrated from pristine PET and prepared nanocomposites into water under various exposure conditions were measured by GC/FID and are displayed in Tables 8, 9, 10 and 11. GC results reveal that dimethyl phthalate (DMP) and dibutyl phthalate (DBP) have greater concentrations in water samples at different conditions. It can be attributed to their smaller molecular sizes, lower molecular weight (Table 4) and their relative polar nature which assist their diffusion and permeation through the PET matrix. Having the highest molar mass, bis 2-ethylhexyl phthalate (DEHP) is not detected at all in the water samples which have been exposed to different nanocomposites at various conditions. However, its presence in water samples in contact with pristine PET was determined, except for the sample that remained at a shorter exposure time (4 weeks) and lower temperature (7 °C). DIBP behaves approximately similar to DEHP with respect to migration from the nanocomposites. DIBP is not detected

in pure PET samples except with longer storage time (6 weeks) and at higher temperature (45 °C).

Although it is expected that DEP concentration in water samples would be more remarkable than DEHP and DIBP due to its lower molecular volume, it was not detected at all in water samples that were in contact with nanocomposites, which may be pertinent to its lower initial concentration in PET. Nevertheless, DEP is well recognized in water that has been in contact with pure PET samples. A representative example of gas chromatographic profile for water sample which is in contact with pristine PET is shown in Fig. 6. It is observed that all the studied phthalate esters are detected in fairly significant amounts in the specified storage condition.

Effect of time on phthalate esters migration

Increasing exposure time causes greater phthalate ester migration from both PET and PET/nanoclay composites under any circumstances according to the results presented in Tables 8, 9, 10 and 11. Even some of the analytes which are not detected after 4 weeks due to their low concentration in water samples are recognized after 6 weeks. In order to understand the role of storage time more comprehensively, Fig. 7a, b shows its effect on concentration of migrated DMP and DBP in water samples at 45 °C, respectively.

In fact, migration phenomena relate to time-dependent factors such as diffusion and permeation. According to Eq. (1) for Fickian diffusion and for short times ($M_t/M_\infty < 0.6$), the square root of time has direct influence on the level of migration:

$$\frac{M_t}{M_\infty} = 4\left(\frac{Dt}{\pi L^2}\right)^{1/2} \tag{1}$$

where, M_t (g/cm^2) is mass transported at time t, M_∞ (g/cm^2) is mass transported at equilibrium, D (cm^2/s) is diffusion coefficient and L (cm) is the film thickness. For longer penetration time ($M_t/M_\infty > 0.6$), the time dependency of migration alters with exponential relation [33]. Studies have confirmed the effect of increasing storage time on enhancing the concentration of migrants [7–9, 34, 35]. Hence, greater migration of analytes into the water with increase in the exposure time is expected. However, comparison of analytes' migration results from PET and PET/clay nanocomposites indicates that the concentration of migrant analytes increases considerably from 4 to 6 weeks for pristine PET while the migrant concentration at the same extended time is much lower for PET/clay nanocomposites.

For instance, the effect of nanoclays on reducing the level of DMP migration at 45 °C with increase in the
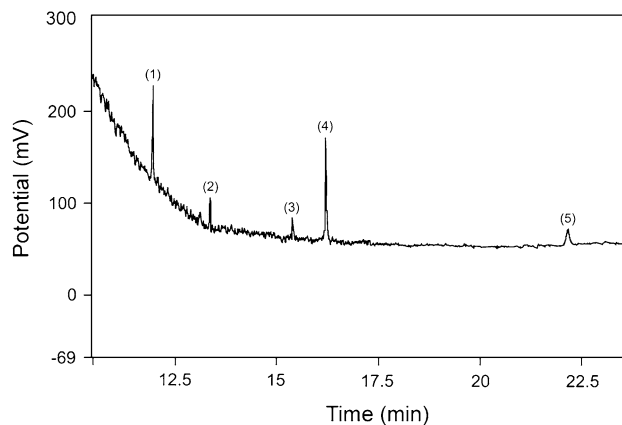

Fig. 6 GC profiles of PET samples in contact with water for 6 weeks at 45 °C: (1) DMP (2) DEP (3) DIBP (4) DBP and (5) DEHP
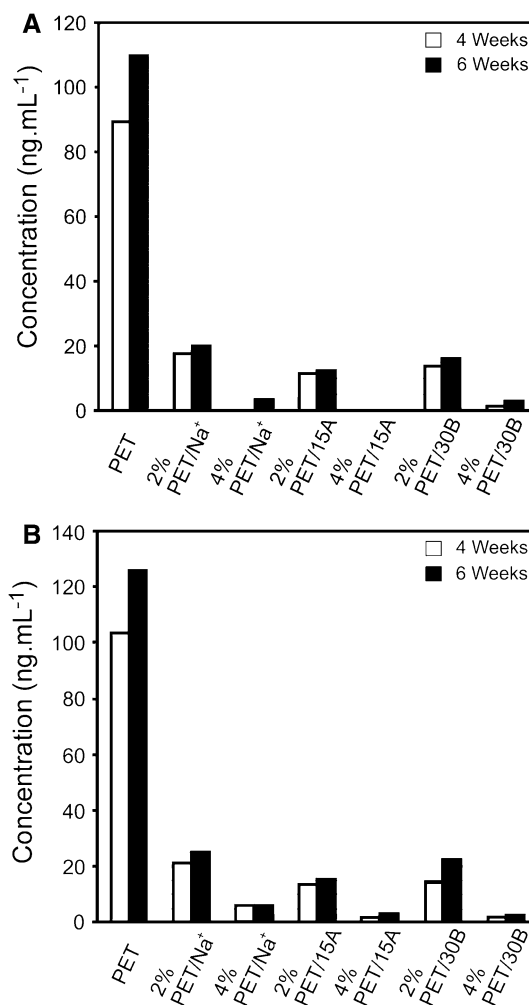

Fig. 7 Concentrations of DMP a and DBP b migrated from PET samples in contact with water at 45 °C and two different exposure times

exposure time is shown in Fig. 7a which confirms the good outcome of applying nanoclay on postponing the migration of the phthalate ester during the storage period. A similar

behavior is observed for other phthalate migrants according to results in Table 8, 9, 10 and 11. DMP exhibits a more increased migration rate compared to DBP due to its smaller molecular size which aids it to diffuse more rapidly.

Thus, it is clarified that nanoclay particles decelerate the migration from PET/nanoclay composites on extending the storage time. The main reason for the mentioned event is based on a theory by Nielsen [36] which states that the existences of the tortuous track around nanoclay sheets in polymer matrix result in longer penetration path for permeating molecules. In this theory, permeability through nanocomposites depends on the tortuous factor (τ) which is the ratio of the detour distance (d') to the thickness of the sample (d) and volume fraction of the filler (φ_s):

$$\tau = \frac{d}{d'} = 1 + \left(\frac{L}{2W}\right)\varphi_s \qquad (2)$$

$$\frac{P_c}{P_p} = \frac{(1 - \varphi_s)}{\tau} \qquad (3)$$

where L/W is the clay particle aspect ratio, and P_c and P_p are permeabilities of nanocomposite and pure polymer, respectively [20]. However, Nielsen just assumed the role of volume fraction of the filler and the nanoclays aspect ratio in his detour theory. Moreover, he supposed that the nanoclay sheets are fully oriented and well dispersed in polymer matrix which differs from actual circumstances. Recently, new models have been proposed to improve the Nielsen model which takes into account parameters such as platelet orientation, constrained polymer region, polymer chain segment immobility factor, plasticization factor, mean diffusion coefficients, and solubility factor that influence the migration rate of permeating molecules[14, 18–20, 23–25, 37]. The presence of more tortuous paths causes lower permeability of analytes at a certain time. If exposure time is extended, more analytes can take a chance to migrate from the packaging materials. However, it would be more difficult in polymer matrixes filled with clay nanoparticles.

Effect of temperature on phthalate ester migration

According to results obtained by GC-FID (Tables 8, 9, 10 and 11), rising temperature leads to the presence of greater amount of phthalate esters in water in both PET and PET/ nanoclay sample. With respect to the results in Table 8, although at the storage temperature of 7 °C DBP was not detected in water samples in contact with PET/Cloisite 30B and PET/Cloisite 15A (4 wt%) nanocomposites, its presence was identified in all aforesaid samples at 45 °C (Table 10). However, the results shown in Fig. 8a, b reveal the markedly lower amount of migrant esters in water
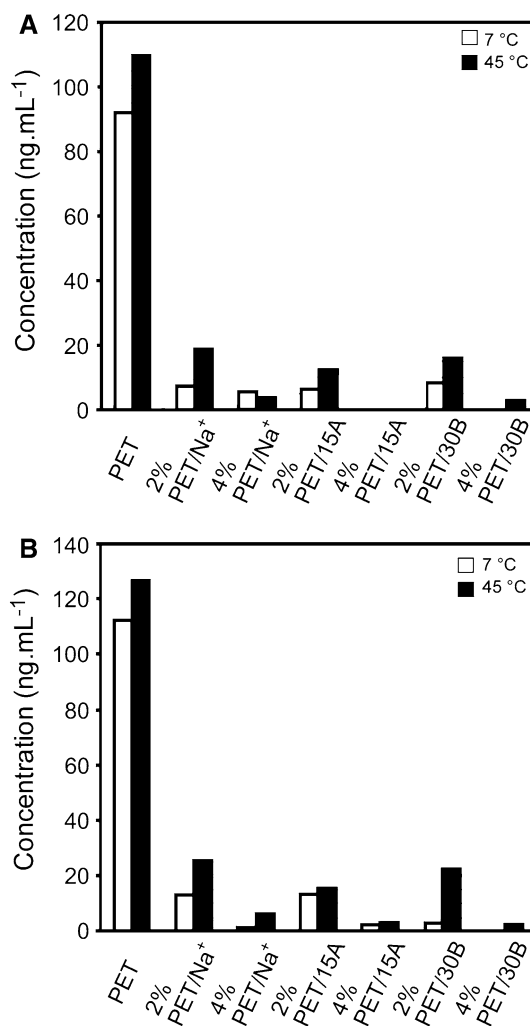

Fig. 8 Concentrations of DMP **a** and DBP **b** migrated from PET samples in contact with water for 6 weeks at two different temperatures

samples which were exposed to PET/nanoclay composites. DMP concentration in water samples which were in contact with pristine PET increased to 17.42 ng mL^{-1} by raising the temperature from 7 to 45 °C, while in the same condition its concentration in water samples increased to 12, 5.91, and 7.61 ng mL^{-1} for PET/Cloisite Na$^+$, PET/Cloisite 15A and PET/Cloisite 30B nanocomposite samples, respectively. These outcomes are attributed to the role of tortuosity provided by nanoclay platelets which resist the migration of phthalate esters from nanocomposite into the water samples even at higher temperatures.

Several studies have reported the effect of rising temperature on the migration rate of by-products, additives and residues from polymers, particularly PET [8, 12, 35, 38]. It should be noticed that the effect of temperature on elevating the level of phthalate ester migration is due to the increase of diffusion coefficient and permeability. It was reported that the diffusion enhancement is due to greater

segmental motions of polymeric chains at higher temperature which results in increase in the size of free volume [39]. In addition, raising the temperature provides the required energy level for chemicals to begin migration [40].

Effect of nanoclay loading on phthalate ester migration

The GC results in Tables 8, 9, 10 and 11 indicate that the increase of nanoclay content results in significant decrease of phthalate esters' presence in water. For instance in Table 11, the amount of dimethyl phthalate (DMP) in water sample decreased from 19.1 to 3.51 ng mL^{-1} on increasing the Cloisite Na$^+$ content in nanocomposite from 2 to 4 wt%, which conveys the great role of clay nanoparticles in reducing the concentration of migrant analyte.

It is also interesting to note that by increasing the Cloisite 15A loading to 4 wt%, DMP was not detected in various water samples under time-temperature conditions (Figs. 7a, 8a). This can be justified by Eqs. (1) and (2) which show the growth of tortuous factor (τ) and subsequently the decline of permeability (P_s) as a result of increase of clay volume fraction (φ_s). Moreover, longer track is a function of high aspect ratio and volume fraction of the clay filler in nanocomposite [14]. Therefore, increasing the filler content would lead to more tortuous longer diffusive path, which retards the phthalate ester migration. In Xu model, higher clay volume fraction decreases the separation gap between clay cuboids with the same thickness in the polymer matrix, which reduces the permeation through the nanocomposite [25].

It is also reported that lower distance between clay plates is seen in nanocomposites with higher clay loading. In this case, the constrained region which may extend to 50-100 nm form the surface of the clay having lower diffusion coefficient compared to bulk pristine polymer dominates the nanocomposite permeation characteristic. The main outcome of the constrained region was to decrease the free volume [18].

In addition, several studies have demonstrated the role of clay particles as nucleating agent and its effect on changing the crystallization rate, which has a direct influence on barrier properties of the nanocomposite [20, 22, 30, 32, 37, 41]. Hence, raising clay volume fraction decreases the diffusion coefficient values and the total chain segment mobility of polymeric matrix. These reductions will be accompanied by a decrease in diffusivity of migrant molecules [20, 25].

Effect of nanoclay type on phthalate esters migration

It is observed that by addition of clay particles regardless of their structure type, the migration of phthalate esters into the water samples is hindered considerably. However, the organically modified nanoclays, Cloisite 30B and Cloisite 15A, exhibit more significant effects on the decrease of migrant concentration in the water samples at various conditions as shown in Tables 8, 9, 10 and 11.

It is believed that the delamination and homogenous distribution of silicate layers increase the tortuosity of the diffusive path throughout the polymeric matrix and thereby migration of analytes is decreased. Individual dispersed platelets of nanoclay in exfoliated structure with higher aspect ratio show improved barrier properties against migrant molecules. Despite having partially exfoliated morphology, PET/Cloisite 30B nanocomposite behaves approximately similar to PET/Cloisite 15A nanocomposite with regard to resisting against permeation. Proper dispersion and distribution of exfoliated Cloisite 30B in polymer matrix is achieved due to intermolecular interactions between hydroxyl groups of nanoclay particles and polar functional groups in PET. However, the results confirm that the lower volume fraction of Cloisite 30B than Cloisite 15A in nanocomposite devalues the effect of tortuous path of its exfoliated structure. Otherwise, for equal volume fraction percentages of both Cloisite 15A and Cloisite 30B in the nanocomposite, the well-dispersed exfoliated structure would definitely exhibit greater barrier properties. Intercalated morphologies with poor dispersion of nanoparticles are achieved by melt mixing of PET and Cloisite 15A for both 2 and 4 wt% nanoclay content. The low capability of intercalation of polymer melts into the Cloisite 15A silicate interlayers relates to the non-polar nature of modified nanoclay platelets that do not have appropriate affinity with the moderate polar PET chains as mentioned earlier on XRD results. In spite of poor dispersion of nanoparticle additives in polymer matrix, the notable resistance against migration of phthalate esters obtained by Cloisite 15A is mainly due to its higher volume fraction in comparison to other nanoclay particles (Table 3).

Among the studied clay particles, non-modified Cloisite Na$^+$ improved the barrier characteristic of the nanocomposite almost less than the other two OMMT. It can be attributed to its lower volume fraction in nanocomposite, besides its lack of tendency to interact with organic polymer chains to form the dispersed morphology. PET chains are also less confined in PET/Cloisite Na$^+$ nanocomposite as compared to PET/Cloisite 30B due to its less dispersed, partially intercalation-exfoliation structure. Alexandre et al. [37] have reported in their study on the polyamide (PA) nanocomposite that Cloisite 30B has lower water sorption than Cloisite Na$^+$ due to the role of the hydrophobic part of the modifier in Cloisite 30B, which induces a considerable decrease in the amount of water adsorption.

Increase of concentration of adsorbed water plasticizes the polymer and creates more free volume for chain

segment mobility, thus enhancing the permeation of migrants. However, water adsorption and swelling of PET is not considerable compared to polar polymers such as PA; thus, greater amount of phthalate esters in water samples in contact with the prepared PET/Cloisite Na$^+$ nanocomposites cannot be referred to as water adsorption. In fact, considering the obtained results, the filler volume fraction and the morphology of clay particles within the PET matrix are the prominent parameters in providing the more tortuous track that directly influences on the level of analyte migration. Therefore, PET/clay nanocomposites with higher clay volume fraction and exfoliated structure would reveal the significant barrier properties.

Conclusion

The migration rate of five major phthalate esters from different PET/nanoclay nanocomposites into the water under various time/temperature conditions were investigated. DSDME coupled with GC/FID was successfully applied for the analysis of ultra-trace levels of phthalate esters in aqueous samples. The proposed method proved to be a simple, quick, precise and highly sensitive procedure and provide good repeatability and reproducibility over a wide linear range. It was observed that PET/Cloisite Na$^+$ samples with 2 wt% of nanoclay content signified the formation of intercalated-exfoliated structure. While content of Cloisite Na$^+$ was raised to 4 wt%, it led to lower extent of exfoliated structures in the nanocomposite. The presence of polar modifiers on Cloisite 30B particles resulted in the delamination of nanoclay platelets and better penetration of PET chains into the interlayer spaces which defined the creation of exfoliated morphology. However, intercalated structure was obtained for PET/Cloisite 15A nanocomposite due to its lack of affinity with moderately polar PET chains. Gas chromatography results confirmed the significant role of nanoclay particles in reducing the migration rate of different phthalate esters in various conditions. As a consequence of the longer tortuous path provided by the nanoclay particles, the migration rate through nanocomposites was noticeably declined. It was also clear that increasing the storage time and temperature highly influenced the diffusion and permeation of migrants. However, with respect to nanoclay particles, the level of phthalate ester migration was not significant in nanocomposites compared to pristine PET even at higher temperature and longer storage time. Raising the nanofiller content in nanocomposites caused a more tortuous, longer diffusive path and reduced the polymer chain segment mobility; hence it postponed the release of phthalate esters in water samples. In brief, it was concluded that the studied Cloisite 30B

and Cloisite 15A exhibit more enhancement of barrier properties, while relatively weaker barrier performance was observed in PET/Cloisite Na$^+$. The outcome for PET/Cloisite Na$^+$ was associated with its lower volume fraction in nanocomposite and its less organophilic nature which led to the partially intercalation-exfoliation of its particles within the PET matrix and consequently lower resistance to phthalate esters migration was attained. The results suggested that continuous monitoring of the PET samples must be implemented, as some phthalate ester concentrations far exceeded the permitted limits. Nanoclay addition relatively retains the level of migrated phthalate esters below the maximum authorized quantity.

References

1. Penalver A, Pocurull E, Borrull F, Marce RM (2000) Determination of phthalate esters in water samples by solid-phase microextraction and gas chromatography with mass spectrometric detection. J Chromatogr A 872:191–201
2. Balafas D, Shaw KJ, Whitfield FB (1999) Phthalate and adipate esters in Australian packaging materials. Food Chem 65:279–287
3. Kim H, Gilbert SG, Johnson JB (1990) Determination of potential migrants from commercial amber polyethylene terephthalate bottle wall. Pharm Res 7:176–179
4. Leivadara SV, Nikolaou AD, Lekkas TD (2008) Determination of organic compounds in bottled waters. Food Chem 108:277–286
5. Prokupková G, Holadovà K, Poustka J, Hajšlovà J (2002) Development of a solid-phase microextraction method for the determination of phthalic acid esters in water. Anal Chim Acta 457:211–223
6. Amiridou D, Voutsa D (2011) Alkylphenols and phthalates in bottled waters. J Hazard Mater 185:281–286
7. Rios JJ, Morales A, Marquez-Ruiz G (2010) Headspace solid-phase microextraction of oil matrices heated at high temperature and phthalate esters determination by gas chromatography multistage mass spectrometry. Talanta 80:2076–2082
8. Schmid P, Kohler M, Meierhofer R, Luzi S, Wegelin M (2008) Does the reuse of PET bottles during solar water disinfection pose a health risk due to the migration of plasticisers and other chemicals into the water? Water Res 42:5054–5060
9. Casajuana N, Lacorte S (2003) Presence and release of phthalic esters and other endocrine disrupting compounds in drinking water. Chromatographia 57:649–655
10. Psillakis E, Kalogerakis N (2003) Hollow-fibre liquid-phase microextraction of phthalate esters from water. J Chromatogr A 999:145–153
11. Cao XL (2008) Determination of phthalates and adipate in bottled water by headspace solid-phase microextraction and gas chromatography/mass spectrometry. J Chromatogr A 1178:231–238
12. Ceretti E, Zani C, Zerbini I, Guzzella L, Scaglia M, Berna V, Donato F, Monarca S, Feretti D (2010) Comparative assessment of genotoxicity of mineral water packed in polyethylene terephthalate (PET) and glass bottles. Water Res 44:1462–1470
13. Lau OW, Wong SK (2000) Contamination in food from packaging material. J Chromatogr A 882:255–270
14. De Azeredo HMC (2009) Nanocomposites for food packaging applications. Food Res Int 42:1240–1253

15. Pollet E, Delcourt C, Alexandre M, Dubois P (2006) Transesterification catalysts to improve clay exfoliation in synthetic biodegradable polyester nanocomposites. Eur Polym J 42:1330–1341

16. Bur AJ, Lee YH, Roth SC, Start PR (2005) Measuring the extent of exfoliation in polymer/clay nanocomposites using real-time process monitoring methods. Polymer 46:10908–10918

17. Ma J, Xu J, Ren JH, Yu ZZ, Mai YW (2003) A new approach to polymer/montmorillonite nanocomposites. Polymer 44:4619–4624

18. Adame D, Beall GW (2009) Direct measurement of the constrained polymer region in polyamide/clay nanocomposites and the implications for gas diffusion. Appl Clay Sci 42:545–552

19. Ray SS, Okamoto M (2003) Polymer/layered silicate nanocomposites: a review from preparation to processing. Prog Polym Sci 28:1539–1641

20. Pavildou S, Papaspyrides CD (2008) A review on polymer–layered silicate nanocomposites. Prog Polym Sci 33:1119–1198

21. Shah RK, Paul DR (2006) Organoclay degradation in melt processed polyethylene nanocomposites. Polymer 47:4075–4084

22. Wang Y, Gao J, Ma Y, Agrawal US (2006) Study on mechanical properties, thermal stability and crystallization behavior of PET/MMT nanocomposites. Compos Part B 37:399–407

23. Lu C, Mai YW (2007) Permeability modelling of polymer-layered silicate nanocomposites. Compos Sci Technol 67:2895–2902

24. Powell CE, Beall GW (2006) Physical properties of polymer/clay nanocomposites. Curr Opin Solid State Mater Sci 10:73–80

25. Xu B, Zheng Q, Song Y, Shangguan Y (2006) Calculating barrier properties of polymer/clay nanocomposites: effects of clay layers. Polymer 47:2904–2910

26. Kim SH, Kim SC (2007) Synthesis and properties of poly(ethylene terephthalate)/clay nanocomposites by in situ polymerization. J Appl Polym Sci 103:1262–1271

27. Sarafraz-Yazdi A, Amiri AH, Eshaghi Z (2009) Separation and determination of benzene, toluene, ethylbenzene and *o*-xylene compounds in water using directly suspended droplet microextraction coupled with gas chromatography-flame ionization detector. Talanta 78:936–941

28. Durmuş A, Woo M, Kasgoz A, Macosko CW, Tsapatsis M (2007) Intercalated linear low density polyethylene (LLDPE)/clay nanocomposites prepared with oxidized polyethylene as a new type compatibilizer: structural, mechanical and barrier properties. Eur Polym J 43:3737–3749

29. Gurmendi U, Eguiazabal JI, Nazabal J (2008) Structure and properties of nanocomposites with a poly(trimethylene terephthalate) matrix. Eur Polym J 44:1686–1695

30. Calcagno CIW, Mariani CM, Teixeira SR, Mauler RS (2007) The effect of organic modifier of the clay on morphology and crystallization properties of PET nanocomposites. Polymer 48:966–974

31. Szép A, Szabo A, Toth N, Anna P, Marosi G (2006) Role of montmorillonite in flame retardancy of ethylene–vinyl acetate copolymer. Polym Degrad Stabil 91:593–599

32. Santos KS, Liberman SA, Oviedo MAS, Mauler RS (2009) Optimization of the mechanical properties of polypropylene-based nanocomposite via the addition of a combination of organoclays. Compos Part A 40:1199–1209

33. Czichos H, Saito T, Smith L (2006) Springer handbook of material measurement methods. Springer, Berlin

34. Monteiro M, Nerin C, Reyes FGR (1999) Migration of Tinuvin P, a UV stabilizer, from PET bottles into fatty-food stimulants. Packag Technol Sci 12:241–248

35. Özlem KE (2008) Acetaldehyde migration from polyethylene terephthalate bottles into carbonated beverages in Türkiye. Int J Food Sci Tech 43:333–338

36. Nielsen LE (1981) Mechanical properties of polymer and composites, vol 2. Marcel Dekker, New York

37. Alexandre B, Langevin D, Mederic P, Aubry T, Couderc H, Nguyen QT, Saiter A, Marais S (2009) Water barrier properties of polyamide 12/montmorillonite nanocomposite membranes: structure and volume fraction effects. J Membrane Sci 328:186–204

38. Graciano-Verdugo AZ, Soto-Valdez H, Peralta E, Cruz-Zarate P, Islas-Rubio AR, Sanches-Valdez S, Sanchez-Escalante A, Gonzalez-Mendez N, Gonzalez-Rios H (2010) Migration of α-tocopherol from LDPE films to corn oil and its effect on the oxidative stability. Food Res Int 43:1073–1078

39. Maiti H, Bhowmick AK (2007) Effect of polymer–clay interaction on solvent transport behavior of fluoroelastomer–clay nanocomposites and prediction of aspect ratio of nanoclay. J Appl Polym Sci 105:435–445

40. Galić K, Ciković N (2001) Permeability characterisation of solvent treated polymer materials. Polym Test 20:599–606

41. Yin M, Li C, Guan G, Zhang D, Xiao YJ (2009) Influence of montmorillonite treatment and montmorillonite dispersion state on the crystallization behavior of poly(ethylene terephthalate)/montmorillonite nanocomposites. J Appl Polym Sci 114:2327–2338